International Institute of Biotechnology and the animals were maintained according to the guidelines for the care of laboratory animals of the Gifu International Institute of Biotechnology.

2.8. Anti-type II collagen antibody-induced arthritis in mice

Inflammatory arthritis was induced using the arthritogenic mouse monoclonal anti-type II collagen 5 clone antibody cocktail (Iwai Chemical, Tokyo, Japan). Seven-weeks-old mice, which were fed with either hydrogen-rich or control water for 2 weeks, were injected intravenously with 1 mg of the arthritogenic cocktail. Hydrogen treatment continued after the injection. Three days later, 25 μg of LPS (*Escherichia coli* O111:B4) was injected intraperitoneally. Two weeks after the antibody injection, we took photographs of the hind and front paws, evaluated the arthritis scores and measured the foot volume of hind paws using the plethysmometer (MK550M, Muromachi-kikai, Tokyo, Japan). The arthritis score was determined by grading each of four paws on a 0–4 scale [12]. Thus, the total arthritis score of a given mouse varies in the range 0–16.

2.9. Statistical analysis

All data were analyzed using Student's *t*-test or two-way ANOVA followed by Fisher's multiple range test.

3. Results

3.1. Hydrogen inhibits LPS/IFNγ-induced NO release from RAW264 macrophage cells

Hydrogen treatment for 24 h did not affect cell viability and proliferation (data not shown). In order to explore possible interaction between NO and hydrogen, we examined the effects of hydrogen on LPS/IFNγ-induced NO release from murine RAW264 macrophage cells. Treatment with hydrogen significantly reduced the NO levels in the culture media, the inhibitory effect being more pronounced at 12 h than at 6 h after LPS/IFNγ stimulation (Fig. 1A). These results suggest that there exists a functional relationship between NO and hydrogen.

3.2. Hydrogen inhibits LPS/IFNγ-induced iNOS expression

Stimulation with LPS/IFNγ up-regulates expression of pro-inflammatory genes such as iNOS and COX2. As shown in Fig. 1B, LPS/IFNγ stimulation resulted in a robust increase in protein expression of iNOS and COX2 at 6 h after treatment, which was markedly suppressed by treatment with hydrogen. Consistent with these findings, quantitative RT-PCR demonstrated that hydrogen inhibits LPS/IFNγ-induced mRNA expression of *iNOS* at 3 h after stimulation (Fig. 1C). These results indicate that hydrogen is capable of inhibiting LPS/IFNγ-induced expression of iNOS, which may account for suppression by hydrogen of LPS/IFNγ-induced NO release from macrophage cells (Fig. 1A).

3.3. Hydrogen inhibits LPS/IFNγ-mediated signal transduction

LPS signaling enhances phosphorylation of MAPKs and IκBα, and thereby activates transcription factors such as AP1, ELK1 and NFκB, whereas IFNγ signaling increases expression of IRF1 via activation of JAK–STAT signaling. These transcription factors activated or up-regulated by LPS/IFNγ stimulation bind to the iNOS promoter and enhance NO production. LPS/IFNγ stimulation enhanced phosphorylation of MAPKs including p38, JNK and ERK as well as AKT and STAT1α (Fig. 2A). Hydrogen treatment inhibited LPS/IFNγ-induced phosphorylation of p38 and JNK, but did not affect that of ERK, AKT and STAT1α.

Phosphorylation of IκB proteins leads to its degradation and NFκB translocation into the nucleus. As shown in Fig. 2B, LPS/IFNγ stimulation enhanced phosphorylation of IκBα and reduced its cytosolic level, which was associated with a decrease in NFκB p65 subunit in the cytosol and its increase in the nuclei. Treatment with hydrogen suppressed the LPS/IFNγ-induced activation of the NFκB pathway.

Taken together, these results suggest that hydrogen suppresses LPS/IFNγ-mediated signal transduction by inhibiting phosphorylation of p38, JNK and IκBα, resulting in reduced iNOS expression and NO production.

3.4. Hydrogen inhibits LPS/IFNγ-induced phosphorylation of ASK1

Among protein kinases activated by LPS/IFNγ, p38, JNK and IκBα were specifically inhibited by hydrogen (Fig. 2A and B). Apoptosis signal-regulating kinase 1 (ASK1), which is activated by endotoxins such as LPS, has been shown to activate both p38 and JNK MAPKs [13]. We thus investigated whether ASK1 phosphorylation is affected by hydrogen. As shown in Fig. 2C, phosphorylation of ASK1 at Ser967 and Thr845 caused by LPS/IFNγ stimulation was attenuated by hydrogen treatment. In contrast, LPS/IFNγ-induced phosphorylation of TGFβ-activated kinase 1 (TAK1) at Ser412 and Thr184/187, which, as well as ASK1, has been implicated in TNF receptor associated factor (TRAF)-dependent signaling pathways [14], was not affected by treatment with hydrogen. These results indicate that hydrogen inhibits LPS/IFNγ-induced phosphorylation of ASK1.

3.5. Hydrogen does not affect LPS/IFNγ-induced NOX activation and ROS production

It has been shown that ASK1 is activated by endotoxins such as LPS through ROS production, which in turn activates p38 and JNK MAPKs [15]. Furthermore, a direct link between ASK1 and NADPH oxidase (NOX) has been reported [16]. Here we investigated whether inhibition by hydrogen of LPS/IFNγ-induced ASK activation is mediated by suppression of NOX activation and ROS production. As shown in Fig. 3A, hydrogen treatment did not affect LPS/IFNγ-induced ROS production. For NOX activation, in response to LPS/IFNγ stimulation, the levels of the cytosolic subunits of NOX, $p47^{phox}$ and $p67^{phox}$, were decreased in the cytosolic fraction and increased in the membrane fraction (Fig. 3B). However, treatment with hydrogen did not influence the LPS/IFNγ-induced translocation of $p47^{phox}$ and $p67^{phox}$ to the membranes. These results suggest that hydrogen does not affect LPS/IFNγ-induced NOX activation and ROS production.

3.6. Oral intake of hydrogen-rich water ameliorates anti-type II collagen antibody-induced arthritis in mice

The findings that hydrogen suppressed LPS/IFNγ-induced NO production in cultured macrophage cells prompted us to examine whether oral intake of hydrogen-rich water could ameliorate anti-type II collagen antibody-induced arthritis in mice, a model for human rheumatoid arthritis [17]. In this mouse disease model, following the injection of anti-type II collagen-specific monoclonal antibody, LPS is injected to increase the incidence and severity of the disease. As shown in Fig. 4A, erythema and swelling of the hind and front paws were alleviated in mice treated with hydrogen-rich water compared with those treated with control water. The arthritis score was significantly lower in hydrogen-rich water-treated mice than in control water-treated mice (Fig. 4B). Both left and right hind paw volumes were decreased in hydrogen-treated mice

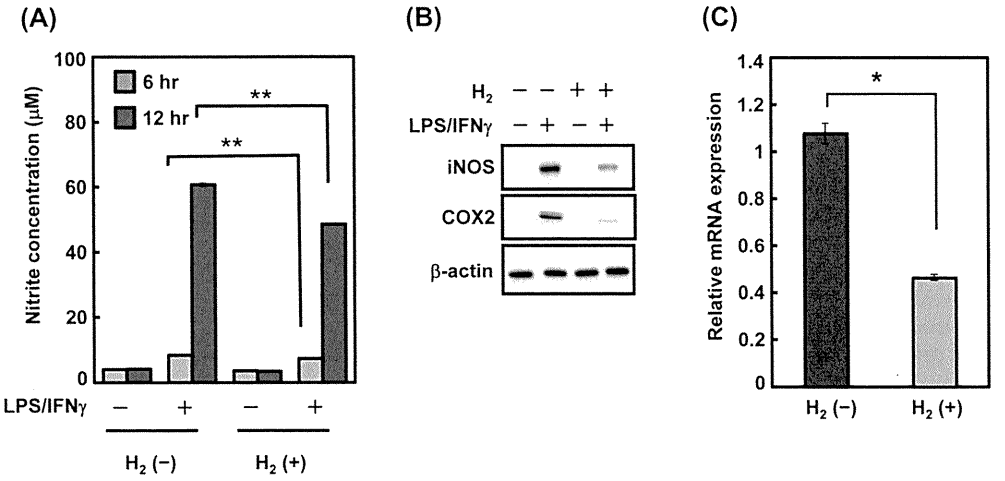

Fig. 1. Effects of hydrogen treatment on LPS/IFNγ-induced NO release and iNOS expression in RAW264 cells. RAW264 cells were incubated for 24 h in the presence or absence of hydrogen and then treated with or without LPS and IFNγ. (A) After incubation in the presence or absence of hydrogen for additional 6 and 12 h, cell culture media were harvested for measurement of nitrite, a stable metabolite of NO (mean ± SD, $n = 9$). Asterisks indicate statistical significance as determined by Student's t-test (**$p < 0.01$). (B) After incubation in the presence or absence of hydrogen for additional 6 h, cell lysates were harvested and subjected to Western blot analysis for iNOS, COX2 and β-actin. A representative blot from three independent experiments is shown. (C) After incubation in the presence or absence of hydrogen for additional 3 h, total RNA was harvested and subjected to quantitative RT-PCR for *iNOS* (mean ± SD, $n = 3$). Asterisks indicate statistical significance as determined by Student's t-test (*$p < 0.05$).

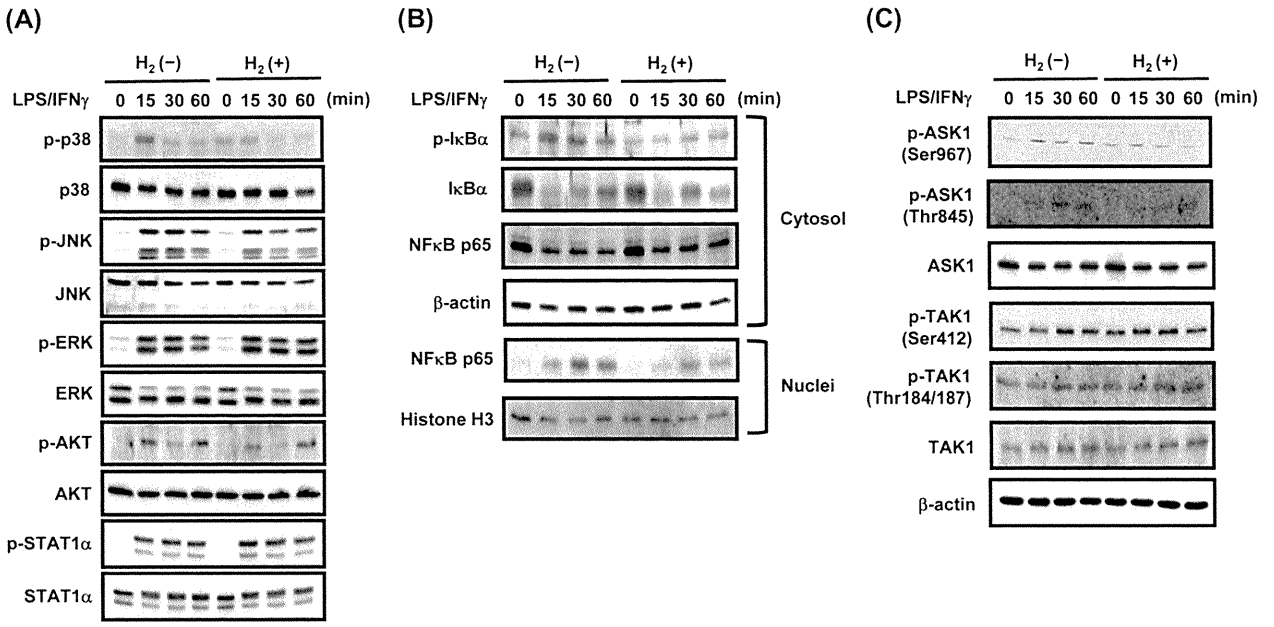

Fig. 2. Effects of hydrogen on LPS/IFNγ-mediated signal transduction in RAW264 macrophage cells. RAW264 macrophage cells were incubated for 24 h in the presence or absence of hydrogen and then treated with or without LPS and IFNγ. After incubation in the presence or absence of hydrogen for indicated time periods, cell lysates (A) and (C) and the cytosolic and nuclear fractions (B) were harvested and subjected to Western blot analysis for indicated proteins. A representative blot from three independent experiments is shown.

compared with control mice, but the statistical significance was observed only for the left hind paw ($p < 0.05$) (Fig. 4C). These results suggest that oral intake of hydrogen-rich water suppresses inflammation and alleviates arthritis in mice.

4. Discussion

Numerous papers have been published showing the efficacy of hydrogen treatment [1] since the first report in 2007 [2], in which specific scavenging of hydroxyl radical has been proposed as a mechanism accounting for the hydrogen effect. Most studies demonstrate reduced oxidative stress by hydrogen and assume that this is a major mechanism underlying the hydrogen effects. However, in type I allergy, hydrogen suppresses phosphorylation of FcεRI-associated Lyn and its downstream signaling molecules, which subsequently inhibits the NOX activity and reduces the generation of hydrogen peroxide [3]. Thus, we concluded that reduction of ROS by hydrogen in type I allergy is the consequence of inhibition of signal transduction, but not of direct radical scavenging activity.

Based on these findings, we hypothesized that hydrogen may ameliorate a wide variety of diseases, irrespective of their causal association with oxidative stress, through modulating yet

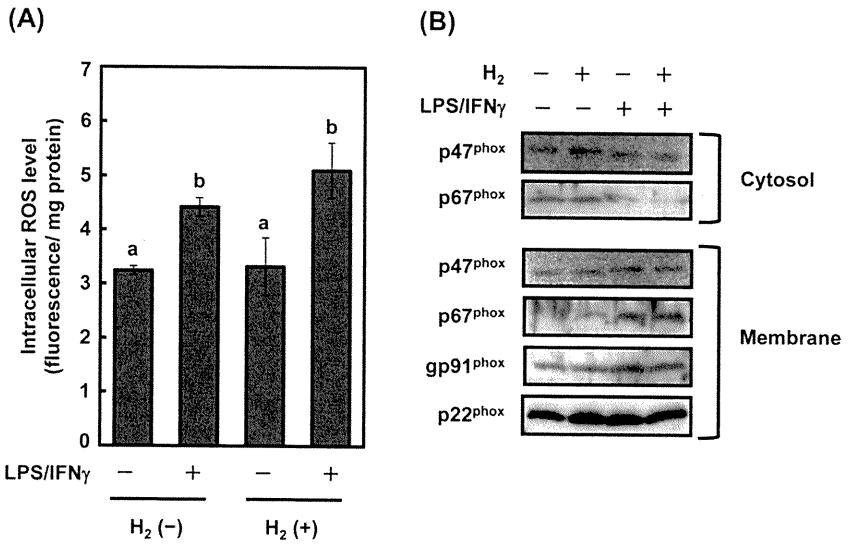

Fig. 3. Effects of hydrogen on LPS/IFNγ-induced NOX activation and ROS production in RAW264 macrophage cells. RAW264 macrophage cells were incubated for 24 h in the presence or absence of hydrogen. (A) Cells were incubated with 10 μM CM-H_2DCF-DA for 1 h in PBS and then treated with or without LPS/IFNγ. Three hours after incubation in the presence or absence of hydrogen, cell lysates were harvested and subjected to measurement of intracellular ROS (mean ± SD, $n = 6$). Statistical significance was determined by two-way ANOVA and Fisher's multiple range test ($p < 0.05$). (B) Cells were treated with or without LPS/IFNγ and then cultured in the presence or absence of hydrogen. Three hours later, the cytosolic and membrane fractions were separated and subjected to Western blot analysis for indicated proteins. A representative blot from three independent experiments is shown.

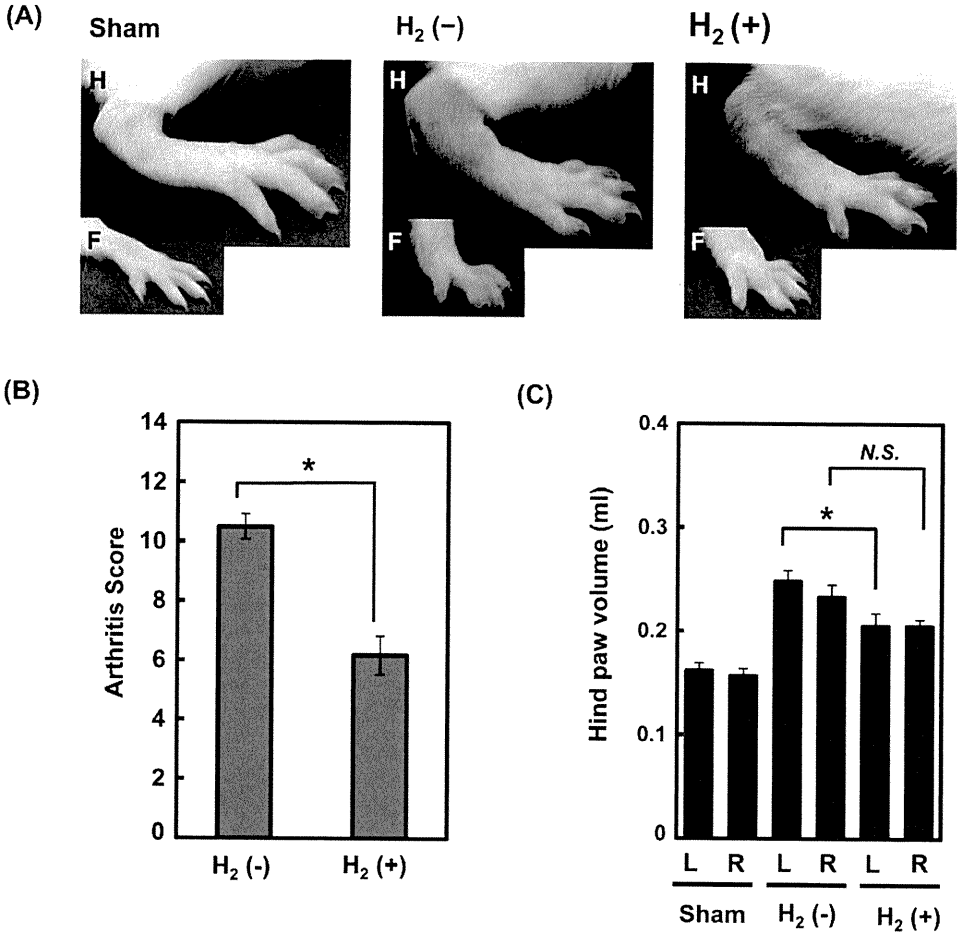

Fig. 4. Effects of oral intake of hydrogen-rich water on anti-type II collagen antibody-induced arthritis in mice. After treatment with or without hydrogen for 2 weeks, BALB/c Cr Slc female mice were injected intravenously with 1 mg of the arthritogenic mouse monoclonal anti-type II collagen antibody cocktail. Three days later, 25 μg of LPS was injected intraperitoneally. Two weeks after the antibody injection, photographs of the hind and front paws were taken (A), the arthritis score was evaluated (B), and the foot volume of hind paws was measured using the plethysmometer (C). Values are expressed as mean ± SD ($n = 5$). Asterisks indicate statistical significance as determined by Student's t-test ($^*p < 0.05$). N.S., not statistically significant; L, left; R, right.

unidentified signaling pathways and also that hydrogen may functionally interact with other gaseous signaling molecule, NO, carbon monoxide (CO) and hydrogen sulfide (H_2S). In an attempt to corroborate our hypotheses, we focused on inflammation because of the following reasons. First, it has been reported that hydrogen alleviates several inflammatory diseases [10,11], the mechanism of which, however, remains unknown. Second, in the inflammatory processes, LPS/IFNγ-induced activation of signal transduction leads to expression of iNOS, resulting in up-regulation of NO.

In the present study, we demonstrated that hydrogen suppresses LPS/IFNγ-induced NO release from macrophage cells (Fig. 1A), which was due to inhibition of LPS/IFNγ-induced expression of iNOS (Fig. 1B and C). We also revealed that LPS/IFNγ-induced phosphorylation of p38, JNK and IκBα was specifically suppressed by hydrogen (Fig. 2A and B). These results suggest that hydrogen may reduce binding to the iNOS promoter of several transcription factors such as AP1 and NFκB via inhibition of signal transduction.

Since our results showed that LPS/IFNγ-induced activation of p38 and JNK is inhibited by hydrogen, we investigated the effects of hydrogen on phosphorylation of ASK1, which is an upstream signaling molecule of both kinases [13]. Indeed, ASK1 phosphorylation was inhibited by hydrogen (Fig. 2C). We also asked if hydrogen directly inhibits phosphorylation of ASK1 *in vitro*, but found that ASK1 phosphorylation is not changed by the presence of hydrogen (Supplementary Fig. 1). On the other hand, ROS-dependent activation of the TRAF6–ASK1–p38 pathway is selectively required for TLR4-mediated innate immunity [15]. In addition, ASK1 is an important effector of NOX in the redox signaling [16]. We thus examined the effects of hydrogen on LPS/IFNγ-induced activation of NOX and subsequent production of ROS, but neither of them was affected by hydrogen treatment (Fig. 3).

In addition to ASK1, hydrogen strongly inhibited the NFκB signaling (Fig. 2B) as represented by a marked decrease in LPS/IFNγ-induced expression of COX2 as well as iNOS (Fig. 1B). In TLR4 signaling, LPS induces interaction of TLR4 with TRAF6, an E3 ubiquitin–protein ligase, and promotes TRAF6 auto-ubiquitination, leading to ubiquitination and activation of TAK1 [18]. TAK1 phosphorylates IκB kinases, which in turn phosphorylate IκB, resulting in IκB degradation and NFκB translocation into the nucleus. TAK1 also activates JNK and p38 MAP kinases by phosphorylating MKK4/7 and MKK3/6, respectively. We therefore investigated if hydrogen could inhibit LPS/IFNγ-induced phosphorylation of TAK1, but TAK1 activation was not affected by treatment with hydrogen (Fig. 2C).

Taken together, we demonstrated that hydrogen inhibits LPS/IFNγ-induced phosphorylation of ASK1 and its downstream signaling molecules (p38 and JNK) as well as IκBα in macrophage cells. Although we were unable to identify the exact molecule(s) that hydrogen directly modulates, we could narrow down the potential target sites. In TLR4 signaling, after formation of the LPS/CD14/TLR4 ligand receptor complex, MyD88 and IRAK as well as TRAF6 and TAK1 are recruited, and their interaction mediates downstream signaling. Our studies suggest that hydrogen modulates molecular events at the receptor or immediately downstream of it. In type I allergy, although the presence of the feed-forward loop in the FcεRI-mediated signal transduction prevented us from identifying direct target(s) of hydrogen, we proposed as a plausible mechanism that hydrogen may compromise the initial step of signal transduction, phosphorylation of Lyn kinase [3]. Together with the findings from the present studies, it is tempting to speculate that molecular hydrogen acts at or around the receptors. Nevertheless, the hypothesis remains to be proved by further studies.

In cultured macrophage cells, we showed that hydrogen inhibits its TLR4 signaling that plays a critical role in induction of pro-inflammatory genes, providing the molecular bases for the hydrogen effects on inflammatory diseases. Finally, we studied *in vivo* effects of hydrogen on inflammation using a mouse model for human rheumatoid arthritis. It was found that oral intake of hydrogen-rich water suppresses inflammation and ameliorates anti-type II collagen antibody-induced arthritis (Fig. 4). Although we and others have demonstrated beneficial effects of hydrogen on inflammatory diseases in animal models, its efficacy in humans needs to be established in clinical trials.

We confirmed that hydrogen is capable of modulating signal transduction and suggested a role for molecular hydrogen as a signal modulator. Since a number of functional interactions among NO, CO and H_2S have been reported [19], it is conceivable that hydrogen may interact with other gas molecules. Indeed, we demonstrated a functional interaction between NO and hydrogen and elucidated the underlying mechanisms. Future studies will provide information about interactions among four gaseous signaling molecules and their physiological significance.

Competing interest statement

The authors declare no conflict of interest.

Acknowledgments

This work was supported by Grant for Biological Research from Gifu prefecture, Japan (Masafumi Ito) and Grants-in-Aid from the Ministry of Education, Culture, Sports, Science, and Technology, Japan (Masafumi Ito).

Appendix A. Supplementary data

Supplementary data associated with this article can be found, in the online version, at doi:10.1016/j.bbrc.2011.06.116.

References

[1] S. Ohta, A. Nakao, K. Ohno, The 2011 Medical Molecular Hydrogen Symposium: An inaugural symposium of the journal Medical Gas Research, Med. Gas Res. 1 (2011) 10.
[2] I. Ohsawa, M. Ishikawa, K. Takahashi, M. Watanabe, K. Nishimaki, K. Yamagata, K. Katsura, Y. Katayama, S. Asoh, S. Ohta, Hydrogen acts as a therapeutic antioxidant by selectively reducing cytotoxic oxygen radicals, Nat. Med. 13 (2007) 688–694.
[3] T. Itoh, Y. Fujita, M. Ito, A. Masuda, K. Ohno, M. Ichihara, T. Kojima, Y. Nozawa, M. Ito, Molecular hydrogen suppresses FcepsilonRI-mediated signal transduction and prevents degranulation of mast cells, Biochem. Biophys. Res. Commun. 389 (2009) 651–656.
[4] C. Bogdan, Nitric oxide and the immune response, Nat. Immunol. 2 (2001) 907–916.
[5] S.B. Abramson, A.R. Amin, R.M. Clancy, M. Attur, The role of nitric oxide in tissue destruction, Best Pract. Res. Clin. Rheumatol. 15 (2001) 831–845.
[6] M.A. Gassull, Review article: the role of nutrition in the treatment of inflammatory bowel disease, Aliment. Pharmacol. Ther. 20 (Suppl. 4) (2004) 79–83.
[7] C. Nathan, Q.W. Xie, Regulation of biosynthesis of nitric oxide, J. Biol. Chem. 269 (1994) 13725–13728.
[8] E.D. Chan, D.W. Riches, IFN-gamma + LPS induction of iNOS is modulated by ERK, JNK/SAPK, and p38(mapk) in a mouse macrophage cell line, Am. J. Physiol. Cell Physiol. 280 (2001) C441–C450.
[9] A.T. Jacobs, L.J. Ignarro, Lipopolysaccharide-induced expression of interferon-beta mediates the timing of inducible nitric-oxide synthase induction in RAW 264.7 macrophages, J. Biol. Chem. 276 (2001) 47950–47957.
[10] K. Xie, Y. Yu, Z. Zhang, W. Liu, Y. Pei, L. Xiong, L. Hou, G. Wang, Hydrogen gas improves survival rate and organ damage in zymosan-induced generalized inflammation model, Shock 34 (2010) 495–501.
[11] M. Kajiya, M.J. Silva, K. Sato, K. Ouhara, T. Kawai, Hydrogen mediates suppression of colon inflammation induced by dextran sodium sulfate, Biochem. Biophys. Res. Commun. 386 (2009) 11–15.
[12] E. Douni, P.P. Sfikakis, S. Haralambous, P. Fernandes, G. Kollias, Attenuation of inflammatory polyarthritis in TNF transgenic mice by diacerein: comparative analysis with dexamethasone, methotrexate and anti-TNF protocols, Arthritis Res. Ther. 6 (2004) R65–R72.
[13] H. Nagai, T. Noguchi, K. Takeda, H. Ichijo, Pathophysiological roles of ASK1-MAP kinase signaling pathways, J. Biochem. Mol. Biol. 40 (2007) 1–6.
[14] M. Landstrom, The TAK1–TRAF6 signalling pathway, Int. J. Biochem. Cell Biol. 42 (2010) 585–589.

[15] A. Matsuzawa, K. Saegusa, T. Noguchi, C. Sadamitsu, H. Nishitoh, S. Nagai, S. Koyasu, K. Matsumoto, K. Takeda, H. Ichijo, ROS-dependent activation of the TRAF6–ASK1–p38 pathway is selectively required for TLR4-mediated innate immunity, Nat. Immunol. 6 (2005) 587–592.
[16] F. Jiang, Y. Zhang, G.J. Dusting, NADPH oxidase-mediated redox signaling: roles in cellular stress response, stress tolerance, and tissue repair, Pharmacol. Rev. 63 (2011) 218–242.
[17] K. Terato, D.S. Harper, M.M. Griffiths, D.L. Hasty, X.J. Ye, M.A. Cremer, J.M. Seyer, Collagen-induced arthritis in mice: synergistic effect of *E. coli* lipopolysaccharide bypasses epitope specificity in the induction of arthritis with monoclonal antibodies to type II collagen, Autoimmunity 22 (1995) 137–147.
[18] C. Wang, L. Deng, M. Hong, G.R. Akkaraju, J. Inoue, Z.J. Chen, TAK1 is a ubiquitin-dependent kinase of MKK and IKK, Nature 412 (2001) 346–351.
[19] M. Kajimura, R. Fukuda, R.M. Bateman, T. Yamamoto, M. Suematsu, Interactions of multiple gas-transducing systems: hallmarks and uncertainties of CO, NO, and H_2S gas biology, Antioxid. Redox Signal. 13 (2010) 157–192.

Ito et al. Medical Gas Research 2011, 1:24
http://www.medicalgasresearch.com/content/1/1/24

MEDICAL GAS RESEARCH

RESEARCH Open Access

Open-label trial and randomized, double-blind, placebo-controlled, crossover trial of hydrogen-enriched water for mitochondrial and inflammatory myopathies

Mikako Ito[1†], Tohru Ibi[2†], Ko Sahashi[3], Masashi Ichihara[4], Masafumi Ito[5] and Kinji Ohno[1*]

Abstract

Background: Molecular hydrogen has prominent effects on more than 30 animal models especially of oxidative stress-mediated diseases and inflammatory diseases. In addition, hydrogen effects on humans have been reported in diabetes mellitus type 2, hemodialysis, metabolic syndrome, radiotherapy for liver cancer, and brain stem infarction. Hydrogen effects are ascribed to specific radical-scavenging activities that eliminate hydroxyl radical and peroxynitrite, and also to signal-modulating activities, but the detailed molecular mechanisms still remain elusive. Hydrogen is a safe molecule that is largely produced by intestinal bacteria in rodents and humans, and no adverse effects have been documented.

Methods: We performed open-label trial of drinking 1.0 liter per day of hydrogen-enriched water for 12 weeks in five patients with progressive muscular dystrophy (PMD), four patients with polymyositis/dermatomyositis (PM/DM), and five patients with mitochondrial myopathies (MM), and measured 18 serum parameters as well as urinary 8-isoprostane every 4 weeks. We next conducted randomized, double-blind, placebo-controlled, crossover trial of 0.5 liter per day of hydrogen-enriched water or placebo water for 8 weeks in 10 patients with DM and 12 patients with MM, and measured 18 serum parameters every 4 weeks.

Results: In the open-label trial, no objective improvement or worsening of clinical symptoms was observed. We, however, observed significant effects in lactate-to-pyruvate ratios in PMD and MM, fasting blood glucose in PMD, serum matrix metalloproteinase-3 (MMP3) in PM/DM, and serum triglycerides in PM/DM. In the double-blind trial, no objective clinical effects were observed, but a significant improvement was detected in lactate in MM. Lactate-to-pyruvate ratios in MM and MMP3 in DM also exhibited favorable responses but without statistical significance. No adverse effect was observed in either trial except for hypoglycemic episodes in an insulin-treated MELAS patient, which subsided by reducing the insulin dose.

Conclusions: Hydrogen-enriched water improves mitochondrial dysfunction in MM and inflammatory processes in PM/DM. Less prominent effects with the double-blind trial compared to the open-label trial were likely due to a lower amount of administered hydrogen and a shorter observation period, which implies a threshold effect or a dose-response effect of hydrogen.

* Correspondence: ohnok@med.nagoya-u.ac.jp
† Contributed equally
[1]Division of Neurogenetics, Center for Neurological Diseases and Cancer, Nagoya University Graduate School of Medicine, 65 Tsurumai, Showa-ku, Nagoya 466-8550, Japan
Full list of author information is available at the end of the article

Background

Ohsawa and colleagues first reported an effect of hydrogen gas on cerebral infarction in June 2007 [1]. Effects of hydrogen administered in the forms of inhaled gas, drinking water, instillation, and intraperitoneal injection have been reported for 31, 4, and 5 diseases in animal models, cells, and humans, respectively [2]. Hydrogen exhibits prominent effects especially on oxidative stress-mediated diseases and inflammatory diseases in rodents. Hydrogen scavenges hydroxyl radicals and less efficiently peroxynitrite [1]. The radical-scavenging activities, however, are unlikely to be an exclusive mechanism, because the amount of radical oxygen species generated in rodents and humans is much more than the amount of hydrogen molecules taken up by the body. Indeed, the amount of hydrogen taken up by drinking hydrogen-enriched water (HEW) is 100 or more times less than that by inhaling 2% hydrogen gas, but drinking HEW exhibits beneficial effects as good as or even better than inhaling 2% hydrogen gas in rodents [2-4], which suggests the lack of a simple dose-response effect. Our previous study on type 1 allergy also indicates that hydrogen suppresses type 1 allergy by acting as a gaseous signal modulator not as a radical scavenger [5].

Effects of hydrogen in humans have been examined in five studies. First, a randomized, double-blind, placebo-controlled crossover study of 900 ml/day of HEW for 8 weeks in 30 patients with diabetes mellitus type 2 demonstrated significant decreases of electronegative charge-modified LDL cholesterol, small dense LDL, and urinary 8-isoprostanes [6]. Second, an open-label trial of electrolyzed hydrogen-enriched hemodialysis solution in 9 patients for 4 months [7] and 21 patients for 6 months [8] showed significant decreases of systolic blood pressure before and after dialysis, as well as of plasma monocyte chemoattractant protein 1 and myeloperoxidase. Third, an open-label trial of 1.5-2.0 liters per day of HEW for 8 weeks in 20 subjects with metabolic syndrome exhibited a 39% increase of urinary superoxide dismutase (SOD), a 43% decrease of urinary thiobarbituric acid reactive substances (TBARS), an 8% increase of high density lipoprotein (HDL)-cholesterol, and a 13% decrease of total cholesterol/HDL-cholesterol ratio [9]. Fourth, a randomized placebo-controlled study of 1.5-2.2 liters/day of HEW for 6 weeks in 49 patients receiving radiotherapy for malignant liver tumors showed marked improvements of QOL scores [10]. As the study was not blinded, subjective QOL scores tended to be overestimated by a placebo effect, but objective markers for oxidative stress were also significantly decreased. Fifth, drip infusion of hydrogen-enriched saline in combination with Edaravone, a clinically approved radical scavenger for cerebral infarction, for 7 days in 8 patients with brain stem infarction was compared to 24 such patients receiving Edaravone alone [11]. Although the study was not randomized and not blinded, MRI markers of patients infused with hydrogen showed significant improvements and accelerated normalization.

Being prompted by the prominent effects of hydrogen on inflammatory diseases and oxidative stress-mediated diseases especially in rodents, we performed an open-label trial of drinking 1.0 liter per day of HEW for 12 weeks in 14 patients with muscle diseases, and identified improvement in four parameters: (i) a decrease of the lactate-to-pyruvate ratio in mitochondrial myopathies (MM) and progressive muscular dystrophy (PMD); (ii) a decrease of serum matrix metalloproteinase-3 (MMP3) in polymyositis/dermatomyositis (PM/DM), (iii) a decrease of fasting glucose in PMD, and (iv) a decrease of serum triglycerides in PM/DM. We then conducted a randomized, double-blind, placebo-controlled, crossover trial of 0.5 liter per day of HEW for 8 weeks in 12 MM and 10 DM cases. We observed that HEW significantly improved serum lactate in MM. In both studies, some patients reported subjective improvement of fatigability, diarrhea, and myalgia, but others reported floating sensation and worsening of diarrhea. We observed no objective improvement or worsening of clinical symptoms during each study. Our studies imply that HEW improves clinical parameters in MM and PM/DM, but 0.5 liter/day for 8 weeks is likely to be insufficient to demonstrate statistically significant effects.

Patients and methods

Patients

For the open-label trial, we recruited 5 patients with PMD, 4 patients with PM/DM, and 5 patients with MM. The PMD patients comprised 1 male with Miyoshi myopathy and 4 females with limb girdle muscular dystrophy type 2B with an average age and SD of 50.4 ± 15.9 years (range 25 - 66). The PM/DM patients comprised 2 males and 2 females with an average age of 53.8 ± 24.8 years (range 29 - 83). All the PM/DM cases were taking 5 - 10 mg of prednisolone per day and were well controlled. The MM patients comprised 4 cases with MELAS (2 males and 2 females with an average age of 45.8 ± 12.3 years, range 37 - 64) and a 54-year-old female with chronic progressive external ophthalmoplegia (CPEO).

For the randomized, double-blind, placebo-controlled, crossover trial, we recruited 12 patients with MM and 10 patients with DM. The MM patients comprised 5 cases with MELAS (2 males and 3 females with an average age of 44.6 ± 17.6 years, range 20 - 65), as well as 7 cases with CPEO (3 males and 4 females with an average age of 49.1 ± 11.1 years, range 29 - 61). The DM patients comprised 3 males and 7 females with an

average age of 49.6 ± 13.7 years (range 32 - 66). All the DM patients were well controlled with 5 - 10 mg prednisolone per day. Three MM and three DM patients participated in both trials. Both trials were approved by the Ethical Review Board of the Aichi Medical University. Informed consent was obtained from each patient.

Protocols

We purchased 500 ml HEW or placebo water in aluminum pouch from Blue Mercury Inc. (Tokyo, Japan). We measured hydrogen concentrations using an H2-N hydrogen needle sensor attached to a PA2000 2-Channel Picoammeter (Unisense Science, Aarhus, Denmark). The hydrogen concentrations were ~0.5 ppm (~31% saturation). We also confirmed that hydrogen in placebo water was undetectable with our system. For each trial, we instructed patients to evacuate the air from the pouch and to close a plastic cap tightly every time after they drink water to keep the hydrogen concentration as high as possible.

For the open-label trial, patients took 1.0 liter per day of HEW in five to ten divided doses for 12 weeks. We measured 18 serum and one urinary parameters and recorded clinical symptoms at 0, 4, 8, 12, 16 weeks.

For the double-blind trial, patients took 0.5 liter per day of HEW or placebo water in two to five divided doses for 8 weeks. Between the 8-week trials with HEW and placebo, we placed a 4-week washout period. We measured 18 serum parameters and recorded clinical symptoms at 0, 4, 8, 12, 16, 20, 24 weeks. In the double-blind trial, we did not measure urinary 8-isoprostane levels.

The data were statistically analyzed using one-way repeated measures ANOVA for the open-label trial and two-way repeated measures ANOVA for the double-blind trial, both followed by the Bonferroni's multiple comparison test using Prism version 4.0c (Graphpad Software, San Diego, CA).

Results

Open-label trial

Fourteen patients with PMD, PM/DM, and MM participated in the study and no patient dropped out of the study. Patients took 1.0 liter of HEW for 12 weeks and we measured 18 serum and one urinary parameters every 4 weeks (Table 1). We observed no objective improvement or worsening of clinical symptoms during the study. All the patients reported increased micturition frequency. Two MELAS patients reported improvement of fatigability, and another MELAS patient complained mild occasional floating sensation. We estimated statistical significance using one-way repeated measures ANOVA analysis and detected five parameters (Figure 1). Serum lactate-to-pyruvate (L/P) ratios of MM patients were high before the study, and were decreased during the study (Figure 1A). Serum L/P ratios and fasting glucose levels of PMD patients were elevated after the study, but the values were still within normal ranges (Figures 1B and 1C). Serum MMP3 levels of DM patients were decreased down to 72.9% of those before HEW, which were again increased after the study (Figure 1D). Serum triglyceride levels of DM patients were elevated after the study (Figure 1E).

Randomized, double-blind, placebo-controlled, crossover trial

Twelve MM and ten DM patients participated in the study and no patient dropped out of the study. Patients took 0.5 liter of HEW or placebo water for 8 weeks and we measured 18 serum parameters every 4 weeks (Table 2). An MM patient reported increased micturition frequency on HEW. A DM patient reported subjective improvement of fatigability and diarrhea on HEW, but an MM patient rather complained increased diarrhea at first on HEW. Another DM patient reported an improvement of myalgia on HEW. A MELAS patient had hypoglycemic episodes only on HEW, but the episodes subsided after the insulin dose was decreased. We observed no objective improvement or worsening of clinical symptoms during the study. Two-way repeated measures ANOVA analysis revealed that only serum lactate levels were significantly decreased in MM by HEW (Figure 2A). Temporal profiles of serum L/P ratios in MM (Figure 2B) and of serum MMP3 levels in DM (Figure 2C) also demonstrated favorable responses to HEW but without statistical significance.

Discussion

We performed open-label and double-blind studies of HEW on myopathic patients. In the open-label study, we observed statistical significance of hydrogen effects in four parameters: L/P ratios in MM and PMD; fasting glucose in PMD; MMP3 in PM/DM; and triglycerides in PM/DM (Figure 1). In the double-blind study, serum lactate levels were significantly improved in MM. L/P ratios in MM and MMP3 in DM were also improved but without statistical significance (Figure 2). Small numbers of participants in both the open-label and double-blind studies might have failed to disclose statistically significant effects of HEW.

In MM, the mitochondrial electron transfer system (mETS) is compromised by mutations in mitochondrial DNA [12]. This results in a decreased influx of NADH into mETS and elevates NADH levels in the cytoplasm, which facilitates conversion of pyruvate to lactate by lactate dehydrogenase. Thus, lactate and L/P ratio are useful surrogate markers to estimate functions of mETS, and are usually abnormally elevated in MM [12]. Defective mETS also causes leakage of electrons from

Table 1 Open-label trial of HEW in 14 myopathic patients

	Progressive muscular dystrophy (PMD)			Polymyositis (PM)/Dermatomyositis (DM)			Mitochondrial myopathies (MM)		
	Before	12 weeks	After	Before	12 weeks	After	Before	12 weeks	After
CK (U/L)	3067 ± 1492	3419 ± 1610	3107 ± 2382	124 ± 31	180 ± 97	140 ± 86	187 ± 75	124 ± 47	156 ± 40
HbA1c (%)	5.25 ± 0.44	5.14 ± 0.31	5.16 ± 0.42	6.68 ± 1.61	6.70 ± 1.53	6.90 ± 2.03	7.40 ± 1.70	7.32 ± 1.48	7.38 ± 1.74
Fasting glucose (mmol/L)	5.52 ± 0.16**	5.51 ± 0.08**	5.82 ± 0.11**	7.66 ± 0.11	7.29 ± 1.57	7.69 ± 1.85	8.94 ± 3.24	9.31 ± 4.18	8.96 ± 3.19
Lactate (mmol/L)	0.95 ± 0.34	1.15 ± 0.40	1.35 ± 0.40	1.42 ± 0.18	1.66 ± 0.32	1.30 ± 0.27	1.84 ± 0.50	1.87 ± 0.78	1.73 ± 0.65
L/P ratio	12.1 ± 0.7*	10.7 ± 1.3*	13.6 ± 2.2*	13.1 ± 0.9	15.0 ± 3.2	12.7 ± 1.0	20.7 ± 2.9*	14.9 ± 3.5*	20.3 ± 3.1*
Creatinine (μmol/L)	34.8 ± 3.1	34.5 ± 6.9	34.7 ± 8.8	58.6 ± 13.7	56.3 ± 10.7	56.6 ± 14.1	48.8 ± 9.0	47.7 ± 9.7	48.6 ± 8.8
BUN (mmol/L)	4.74 ± 1.16	4.20 ± 0.60	4.21 ± 1.05	4.33 ± 0.71	4.11 ± 0.48	4.68 ± 0.74	5.28 ± 1.69	5.89 ± 1.09	5.00 ± 1.58
Uric acid (μmol/dL)	295 ± 46	315 ± 61	300 ± 30	319 ± 44	331 ± 71	329 ± 40	208 ± 50	220 ± 60	217 ± 45
Urinary 8-isoprostane (ng/mg Cr)	303 ± 155	392 ± 173	n.d.	222 ± 88	237 ± 86	n.d.	274 ± 117	261 ± 59	n.d.
T-chol (mmol/L)	5.42 ± 0.99	5.74 ± 1.02	5.70 ± 0.81	5.28 ± 0.31	5.55 ± 0.93	5.97 ± 1.35	4.52 ± 0.75	4.53 ± 0.34	4.42 ± 0.77
LDL-chol (mmol/L)	3.30 ± 1.05	2.86 ± 1.46	2.99 ± 1.15	2.66 ± 0.28	3.21 ± 0.99	3.13 ± 1.02	2.44 ± 0.43	2.27 ± 0.44	2.22 ± 0.45
HDL-chol (mmol/L)	1.62 ± 0.21	1.49 ± 0.19	1.62 ± 0.18	2.01 ± 0.73	1.99 ± 0.76	2.02 ± 0.67	1.14 ± 0.79	1.03 ± 0.72	1.04 ± 0.69
Triglycerides (mmol/L)	1.31 ± 0.46	3.62 ± 4.83	3.07 ± 3.67	2.17 ± 0.63*	2.01 ± 1.21*	3.09 ± 1.22*	0.78 ± 0.34	0.89 ± 0.45	0.73 ± 0.37
WBC (10^9/L)	5.30 ± 1.32	5.40 ± 1.12	4.80 ± 0.38	10.78 ± 2.08	8.35 ± 3.41	10.10 ± 0.17	5.12 ± 1.27	7.27 ± 2.29	5.93 ± 1.35
RBC (10^{12}/L)	4.17 ± 0.64	3.79 ± 0.42	3.87 ± 0.80	4.01 ± 0.62	4.34 ± 0.36	4.49 ± 0.45	4.33 ± 0.43	4.31 ± 0.78	4.35 ± 0.59
Platelets (10^9/L)	262 ± 42	260 ± 33	270 ± 20	337 ± 123	265 ± 82	270 ± 65	215 ± 25	207 ± 28	217 ± 25
Hematocrit	0.375 ± 0.040	0.374 ± 0.038	0.407 ± 0.055	0.337 ± 0.069	0.376 ± 0.041	0.395 ± 0.045	0.381 ± 0.036	0.370 ± 0.047	0.378 ± 0.038
MMP3 (ng/ml)	n.d.	n.d.	n.d.	307.8 ± 59.1*	224.3 ± 53.4*	283.3 ± 77.6*	n.d.	n.d.	n.d.
IgG (mg/dl)	n.d.	n.d.	n.d.	1343 ± 470	1396 ± 550	1429 ± 581	n.d.	n.d.	n.d.

Values represent mean ± SD. n.d., not determined. *$p < 0.05$ and **$p < 0.005$ by one-way repeated measures ANOVA.

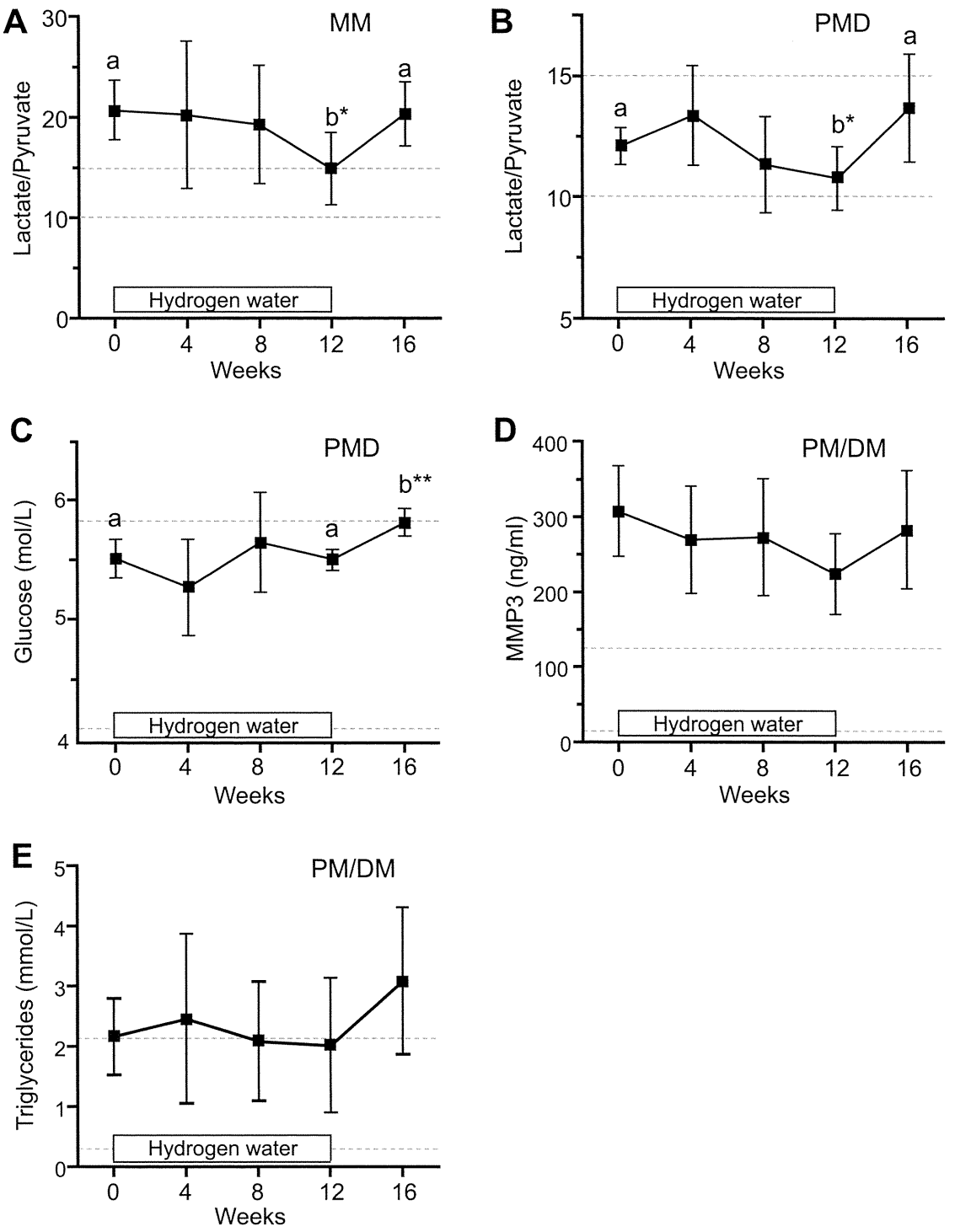

Figure 1 Temporal profiles of four parameters that demonstrate statistical significance by one-way repeated measures ANOVA in the open-label trial. Ratios of serum lactate/pyruvate (L/P) in 5 mitochondrial myopathies (MM) patients **(A)** and 4 progressive muscular dystrophy (PMD) patients **(B)**. Note abnormally high L/P ratios in MM patients. **(C)** Fasting glucose in 4 PMD patients. **(D)** Serum MMP3 in 5 Polymyositis (PM)/Dermatomyositis (DM) patients. **(E)** Serum triglycerides in 4 PMD patients. Twelve weeks on HEW are indicated by a box in each panel. Means and SD are plotted. Statistically different values by the Bonferroni's multiple comparison test are indicated by 'a' and 'b' with *$p < 0.05$ and **$p < 0.01$. Bonferroni's test reveal no statistical difference between any two values in **(D)** and **(E)**. Broken lines show a normal range of each parameter.

Table 2 Randomized, double-blind, placebo-controlled, crossover trial of HEW in 10 DM and 12 MM patients

	Dermatomyositis (DM)				Mitochondrial myopathies (MM)			
	Hydrogen water		Placebo water		Hydrogen water		Placebo water	
	0 week	8 weeks	0 week	8 weeks	0 week	8 weeks	0 week	8 weeks
CK (U/L)	88.7 ± 24.3	106.1 ± 88.2	93.5 ± 45.0	99.5 ± 86.7	165 ± 86.6	120 ± 55.5	142.0 ± 69.4	221 ± 235
HbA1c (%)	6.23 ± 1.28	6.34 ± 1.55	6.27 ± 1.44	6.16 ± 1.28	6.09 ± 0.94	6.12 ± 1.05	6.06 ± 1.22	6.06 ± 1.02
Fasting glucose (mmol/L)	8.27 ± 3.62	7.81 ± 2.91	6.70 ± 2.11	6.48 ± 1.90	6.05 ± 1.43	5.67 ± 1.99	6.02 ± 1.46	6.11 ± 1.69
Lactate (mmol/L)	1.93 ± 0.78	1.81 ± 0.87	1.80 ± 0.89	1.65 ± 0.77	1.76 ± 0.67*	1.61 ± 0.48*	1.49 ± 0.49*	1.70 ± 0.57*
L/P ratio	13.1 ± 6.0	11.5 ± 2.6	12.1 ± 2.88	15.2 ± 8.3	18.7 ± 8.8	17.9 ± 7.7	7.12 ± 13.4	17.7 ± 8.6
Creatinine (μmol/L)	59.1 ± 15.6	59.1 ± 13.6	58.3 ± 15.0	59.0 ± 19.7	53.6 ± 18.3	52.0 ± 17.4	54.8 ± 20.3	57.5 ± 22.3
BUN (mmol/L)	5.36 ± 1.48	4.82 ± 1.57	5.78 ± 1.71	4.86 ± 1.56	6.08 ± 2.09	5.39 ± 1.54	6.24 ± 1.46	6.34 ± 2.76
Uric Acid (μmol/dL)	303 ± 88	320 ± 68	313 ± 75	321 ± 83	413 ± 316	375 ± 229	447 ± 387	408 ± 284
T-chol (mmol/L)	5.23 ± 0.78	5.15 ± 0.85	5.21 ± 0.61	4.95 ± 0.92	4.61 ± 0.78	4.80 ± 0.57	4.69 ± 0.78	4.68 ± 0.71
LDL-chol (mmol/L)	3.06 ± 0.82	2.93 ± 0.75	2.97 ± 0.80	3.03 ± 0.84	2.69 ± 0.68	2.82 ± 0.58	2.73 ± 0.67	2.79 ± 0.60
HDL-chol (mmol/L)	1.59 ± 0.48	1.56 ± 0.36	1.53 ± 0.47	1.43 ± 0.48	1.47 ± 0.04	1.55 ± 0.34	1.52 ± 0.34	1.45 ± 0.35
Triglycerides (mmol/L)	1.54 ± 0.65	1.83 ± 0.76	1.86 ± 0.80	1.85 ± 0.48	1.16 ± 0.58	0.92 ± 0.35	0.97 ± 0.36	1.02 ± 0.49
WBC (10^9/L)	11.7 ± 6.4	10.9 ± 3.1	9.66 ± 2.68	11.2 ± 4.7	5.5 ± 0.1	5.7 ± 1.8	5.81 ± 1.78	5.8 ± 1.9
RBC (10^{12}/L)	4.28 ± 0.05	4.32 ± 0.35	4.37 ± 0.44	4.35 ± 0.44	4.15 ± 0.04	4.17 ± 0.61	4.26 ± 0.67	4.15 ± 0.56
Platelets (10^9/L)	271 ± 10	302 ± 69	306 ± 54	312 ± 79	203 ± 40	214 ± 44	216 ± 48	225 ± 50
Hematocrit (%)	0.380 ± 0.004	0.384 ± 0.040	0.392 ± 0.052	0.391 ± 0.047	0.373 ± 0.004	0.378 ± 0.060	0.386 ± 0.063	0.376 ± 0.058
MMP3 (ng/ml)	245 ± 122	232 ± 84.1	217 ± 93.5	221 ± 112	n.d.	n.d.	n.d.	n.d.
IgG (mg/dl)	1211 ± 357	1244 ± 305	1202 ± 340	1282 ± 353	n.d.	n.d.	n.d.	n.d.

Values represent mean ± SD. n.d., not determined. *p < 0.05 by two-way repeated measures ANOVA.

mitochondrial inner membranes and increases production of reactive oxygen species (ROS), which further damages mETS [13,14]. Reduction of the L/P ratios in the open-label and double-blind studies suggests that hydrogen alleviates mETS dysfunction in MM either by scavenging ROS or by yet unidentified signaling mechanisms.

MMP3 belongs to a family of calcium-dependent zinc proteinases induced by cytokines and secreted by inflammatory cells. MMPs enhance T-cell migration and adhesion, and also degrade the extracellular matrix proteins [15]. MMP3 is increased in a fraction of DM patients [16]. MMP3 may facilitate lymphocyte adhesion and enhance T-cell-mediated cytotoxicity by degrading extracellular matrix proteins in DM. Hydrogen improved serum MMP3 levels in the open-label and double-blind studies, which is expected to ameliorate pathogenic inflammatory processes that culminates in muscle fiber destruction.

We observed less prominent effects with the double-blind study compared to the open-label study. The lack of statistically significance in the double-blind study is possibly due to a lower amount of HEW (1.0 vs. 0.5 liter per day) and to a shorter observation period (12 vs. 8 weeks). In the open-label study, drinking 1.0 liter of HEW was not readily accommodated by most myopathic patients. Hydrogen does not show simple dose-response relationship in rodents [2-4], and *ad libitum* administration of even 5%-saturated HEW markedly attenuates development of Parkinson's disease in mice [17]. We thus reduced the amount of hydrogen to 0.5 liter in the double-blind trial, and also shortened the observation period to minimize the burden on the participants. This, however, might have masked effects of HEW. Indeed, when we compare studies of diabetes mellitus type 2 [6], the current open-label trial, and metabolic syndrome [9], the participants took 0.9, 1.0, and 1.5-2.0 liters of HEW, respectively. Ratios of total cholesterol/HDL-cholesterol are available at 8 weeks in all the studies, and are changed to 103.8%, 98.6%, and 95.8%, respectively, of those before hydrogen administration, which is in accordance with a dose-response effect of HEW. Additionally, among the two previous studies [6,9] and the current open-label and double-blind studies, the most prominent effects are observed with 1.5-2.0 liters of HEW. As drinking a large amount of HEW is not easily accommodated by most patients especially in winter, a threshold effect and/or a dose-response effect should be further elaborated for each pathological state.

Conclusions

HEW is effective for mitochondrial dysfunction in MM and inflammatory processes in DM. Hydrogen may have

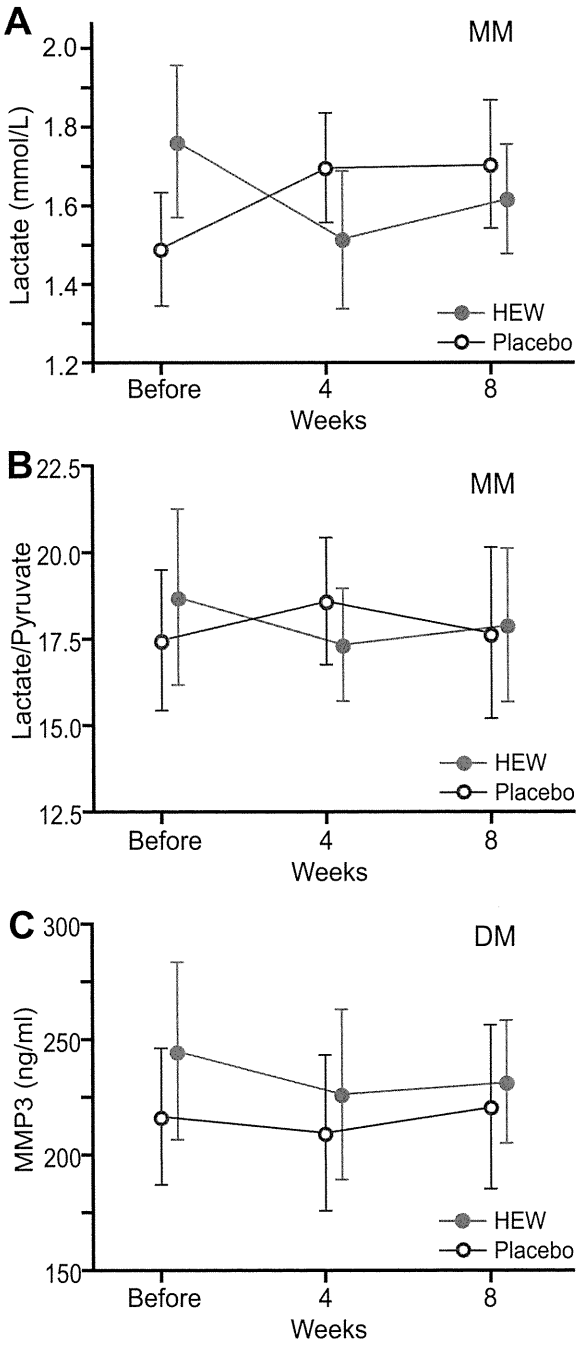

Figure 2 Temporal profiles of three parameters in the double-blind trial. Serum lactate **(A)** and L/P ratios **(B)** in 12 mitochondrial myopathies (MM) patients. **(C)** Serum MMP3 in 10 dermatomyositis (DM) patients. Patients took HEW or placebo for 8 weeks. Means and SD are plotted. **(A)** Serum lactate levels in MM are statistically different by two-way repeated measures ANOVA ($p < 0.05$, Table 1), but the Bonferroni's multiple comparison test reveals no statistical difference between any two values. No statistical difference was observed in L/P ratios **(B)** and serum MMP3 **(C)**. The normal range of lactate is 0.5-2.2 mmol/l. Normal ranges of the other parameters are indicated in Figure 1.

a threshold effect or a dose-response effect and 1.0 liter or more per day of HEW is likely to be required to exert beneficial effects.

Abbreviations

HEW: hydrogen-enriched water; PMD: progressive muscular dystrophy; PM: polymyositis; DM: dermatomyositis; MM: mitochondrial myopathies; CPEO: chronic progressive external ophthalmoplegia; MELAS: mitochondrial myopathy with lactic acidosis and stroke-like episodes; MMP3: matrix metalloproteinase-3.

Acknowledgements

We would like to thank the patients for their participation in these studies. We thank Fumiko Ozawa for her technical assistance. This work was supported by Grants-in-Aid from the Ministry of Health, Labor, and Welfare of Japan and the Ministry of Education, Culture, Sports, Science, and Technology of Japan.

Author details

[1]Division of Neurogenetics, Center for Neurological Diseases and Cancer, Nagoya University Graduate School of Medicine, 65 Tsurumai, Showa-ku, Nagoya 466-8550, Japan. [2]Faculty of Pathophysiology and Therapeutics, Aichi Medical University College of Nursing, 21 Karimata Yazako, Nagakute-cho, Aichi-gun, Aichi 480-1195, Japan. [3]Department of Neurology, Aichi Medical University School of Medicine, 21 Karimata Yazako, Nagakute-cho, Aichi-gun, Aichi 480-1195, Japan. [4]Department of Biomedical Sciences, College of Life and Health Sciences, Chubu University, 1200 Matsumoto, Kasugai, Aichi 487-8501, Japan. [5]Department of Longevity and Aging Research, Gifu International Institute of Biotechnology, 1-1 Nakafudogaoka, Kakamigahara, Gifu 504-0838, Japan.

Authors' contributions

TI and KS examined patients and acquired data. MI[1] and TI organized data and performed statistical analysis. MI[1] and KO wrote the paper. MI[4], MI[5], and KO conceived the study. All authors read and approved the final manuscript.

Competing interests

The authors declare that they have no competing interests.

Received: 24 June 2011 Accepted: 3 October 2011
Published: 3 October 2011

References

1. Ohsawa I, Ishikawa M, Takahashi K, Watanabe M, Nishimaki K, Yamagata K, Katsura K, Katayama Y, Asoh S, Ohta S: **Hydrogen acts as a therapeutic antioxidant by selectively reducing cytotoxic oxygen radicals.** *Nat Med* 2007, **13**:688-694.
2. Ohta S, Nakao A, Ohno K: **The 2011 Medical Molecular Hydrogen Symposium: An Inaugural Symposium of the Journal Medical Gas Research.** *Med Gas Res* 2011, **1**:10.
3. Nakao A, Sugimoto R, Billiar TR, McCurry KR: **Therapeutic Antioxidant Medical Gas.** *J Clin Biochem Nutr* 2009, **44**:1-13.
4. Hong Y, Chen S, Zhang JM: **Hydrogen as a selective antioxidant: a review of clinical and experimental studies.** *J Int Med Res* 2010, **38**:1893-1903.
5. Itoh T, Fujita Y, Ito M, Masuda A, Ohno K, Ichihara M, Kojima T, Nozawa Y, Ito M: **Molecular hydrogen suppresses FcepsilonRI-mediated signal transduction and prevents degranulation of mast cells.** *Biochem Biophys Res Commun* 2009, **389**:651-656.
6. Kajiyama S, Hasegawa G, Asano M, Hosoda H, Fukui M, Nakamura N, Kitawaki J, Imai S, Nakano K, Ohta M, Adachi T, Obayashi H, Yoshikawa T: **Supplementation of hydrogen-rich water improves lipid and glucose metabolism in patients with type 2 diabetes or impaired glucose tolerance.** *Nutr Res* 2008, **28**:137-143.
7. Nakayama M, Kabayama S, Nakano H, Zhu WJ, Terawaki H, Nakayama K, Katoh K, Satoh T, Ito S: **Biological Effects of Electrolyzed Water in Hemodialysis.** *Nephron Clin Pract* 2009, **112**:C9-C15.
8. Nakayama M, Nakano H, Hamada H, Itami N, Nakazawa R, Ito S: **A novel bioactive haemodialysis system using dissolved dihydrogen (H-2)**

produced by water electrolysis: a clinical trial. *Nephrol Dial Transplant* 2010, **25**:3026-3033.

9. Nakao A, Toyoda Y, Sharma P, Evans M, Guthrie N: **Effectiveness of Hydrogen Rich Water on Antioxidant Status of Subjects with Potential Metabolic Syndrome-An Open Label Pilot Study.** *J Clin Biochem Nutr* 2010, **46**:140-149.
10. Kang K-M, Kang Y-N, Choi I-B, Gu Y, Kawamura T, Toyoda Y, Nakao A: **Effects of drinking hydrogen-rich water on the quality of life of patients treated with radiotherapy for liver tumors.** *Med Gas Res* 2011, **1**:11.
11. Ono H, Nishijima Y, Adachi1 N, Tachibana S, Chitoku S, Mukaihara S, Sakamoto M, Kudo Y, Nakazawa J, Kaneko K, Nawashiro H: **Improved brain MRI indices in the acute brain stem infarct sites treated with hydroxyl radical scavengers, Edaravone and hydrogen, as compared to Edaravone alone. A non-controlled study.** *Med Gas Res* 2011, **1**:12.
12. DiMauro S: **Pathogenesis and treatment of mitochondrial myopathies: recent advances.** *Acta Myologica* 2010, **29**:333-338.
13. Wei YH, Lu CY, Wei CY, Ma YS, Lee HC: **Oxidative stress in human aging and mitochondrial disease-consequences of defective mitochondrial respiration and impaired antioxidant enzyme system.** *Chin J Physiol* 2001, **44**:1-11.
14. McKenzie M, Liolitsa D, Hanna MG: **Mitochondrial disease: mutations and mechanisms.** *Neurochem Res* 2004, **29**:589-600.
15. Sternlicht MD, Werb Z: **How matrix metalloproteinases regulate cell behavior.** *Annu Rev Cell Dev Biol* 2001, **17**:463-516.
16. Nishijima C, Hayakawa I, Matsushita T, Komura K, Hasegawa M, Takehara K, Sato S: **Autoantibody against matrix metalloproteinase-3 in patients with systemic sclerosis.** *Clin Exp Immunol* 2004, **138**:357-363.
17. Fujita K, Seike T, Yutsudo N, Ohno M, Yamada H, Yamaguchi H, Sakumi K, Yamakawa Y, Kido MA, Takaki A, Katafuchi T, Nakabeppu Y, Noda M: **Hydrogen in drinking water reduces dopaminergic neuronal loss in the 1-methyl-4-phenyl-1,2,3,6-tetrahydropyridine mouse model of Parkinson's disease.** *PLoS One* 2009, **4**:e7247.

doi:10.1186/2045-9912-1-24
Cite this article as: Ito *et al.*: Open-label trial and randomized, double-blind, placebo-controlled, crossover trial of hydrogen-enriched water for mitochondrial and inflammatory myopathies. *Medical Gas Research* 2011 1:24.

Hum Genet (2011) 130:671–683
DOI 10.1007/s00439-011-1006-9

ORIGINAL INVESTIGATION

Hyperuricemia cosegregating with osteogenesis imperfecta is associated with a mutation in *GPATCH8*

Hiroshi Kaneko · Hiroshi Kitoh · Tohru Matsuura · Akio Masuda · Mikako Ito · Monica Mottes · Frank Rauch · Naoki Ishiguro · Kinji Ohno

Received: 28 February 2011 / Accepted: 9 May 2011 / Published online: 19 May 2011

Abstract Autosomal dominant osteogenesis imperfecta (OI) is caused by mutations in *COL1A1* or *COL1A2*. We identified a dominant missense mutation, c.3235G>A in *COL1A1* exon 45 predicting p.G1079S, in a Japanese family with mild OI. As mutations in exon 45 exhibit mild to lethal phenotypes, we tested if disruption of an exonic splicing *cis*-element determines the clinical phenotype, but detected no such mutations. In the Japanese family, juvenile-onset hyperuricemia cosegregated with OI, but not in the previously reported Italian and Canadian families with c.3235G>A. After confirming lack of a founder haplotype in three families, we analyzed *PRPSAP1* and *PRPSAP2* as candidate genes for hyperuricemia on chr 17 where *COL1A1* is located, but found no mutation. We next resequenced the whole exomes of two siblings in the Japanese family and identified variable numbers of previously reported hyperuricemia-associated SNPs in *ABCG2* and *SLC22A12*. The same SNPs, however, were also detected in normouricemic individuals in three families. We then identified two missense SNVs in *ZPBP2* and *GPATCH8* on chromosome 17 that cosegregated with hyperuricemia in the Japanese family. *ZPBP2* p.T69I was at the non-conserved region and was predicted to be benign by *in silico* analysis, whereas *GPATCH8* p.A979P was at a highly conserved region and was predicted to be deleterious, which made p.A979P a conceivable candidate for juvenile-onset hyperuricemia. *GPATCH8* is only 5.8 Mbp distant from *COL1A1* and encodes a protein harboring an RNA-processing domain and a zinc finger domain, but the molecular functions have not been elucidated to date.

Electronic supplementary material The online version of this article (doi:10.1007/s00439-011-1006-9) contains supplementary material, which is available to authorized users.

H. Kaneko · T. Matsuura · A. Masuda · M. Ito · K. Ohno (✉)
Division of Neurogenetics, Center for Neurological Diseases and Cancer, Nagoya University Graduate School of Medicine, 65 Tsurumai, Showa-ku, Nagoya 466-8550, Japan
e-mail: ohnok@med.nagoya-u.ac.jp

H. Kaneko · H. Kitoh · N. Ishiguro
Department of Orthopaedic Surgery, Nagoya University Graduate School of Medicine, Nagoya, Japan

M. Mottes
Department of Life and Reproduction Sciences, University of Verona, Verona, Italy

F. Rauch
Genetics Unit, Shriners Hospital for Children and McGill University, Montreal, QC, Canada

Introduction

Osteogenesis imperfecta (OI) is a heritable connective tissue disorder characterized by bone fragility and low bone mass. Clinical severities are widely variable ranging from intrauterine fractures and perinatal lethality to very mild forms without fractures. Patients also exhibit associated features including blue sclera, dentinogenesis imperfecta, hyperlaxity of ligaments and skin, and hearing loss (Rauch and Glorieux 2004). The widely used classification initially described by Sillence et al. (1979) distinguishes types I, II, III and IV (MIM# 166200, 166210, 259420, and 166220, respectively) on the basis of clinical and radiographic findings. Recently, five additional types of V, VI, VII, VIII and IX (MIM# 610967, 610968, 610682, 610915, and 259440, respectively) have been reported (Cabral et al. 2007; Glorieux et al. 2000, 2002; van Dijk et al. 2009; Ward et al. 2002). OI type I is the mildest form characterized by fractures with little or no limb deformity and

normal or mildly short stature, whereas type II is a perinatal lethal form, mostly due to respiratory failure resulting from multiple rib fractures. Type III is characterized by progressive deformities and fractures that are often present at birth. Severities of types IV, V, VI and VII are between those of types I and III. Type VIII and IX carry features of both types II and III.

Type I collagen is the most abundant bone protein. Most patients (>90%) with OI types I–IV have dominant or recessive mutation(s) in either of two genes, *COL1A1* (MIM# 120150) on chromosome (chr) 17q21.31–q22 and *COL1A2* (MIM# 120160) on chr 7q22.1 that encode the α1 and α2 chains of type I procollagen, respectively (Rauch and Glorieux 2004). A genetic cause of type V remains undetermined to date. Types VI to IX are caused by recessive mutations. Type VI is caused by mutations in *FKBP10* (MIM# 607063) encoding FK506-binding protein 65 (FKBP65) that is a chaperone in type I procollagen folding (Alanay et al. 2010). Type VII is caused by mutations in *CRTAP* (MIM# 605497) encoding cartilage-associated protein (CRTAP) (Morello et al. 2006). Type VIII is caused by mutations in *LEPRE1* (MIM# 610339) encoding prolyl 3-hydroxylase 1 (P3H1) (Cabral et al. 2007). Type IX is caused by mutations in *PPIB* (MIM# 123841) encoding cyclophilin B (CYPB) (van Dijk et al. 2009). CRTAP, P3H1 and CYPB form an intracellular collagen-modifying complex that 3-hydroxylates proline at position 986 in the α1 chain of type I collagen, which is essential for correct folding and stability of the collagen triple helix. Mutations in *CRTAP* and *LEPRE1* are also identified in severe OI phenotypes including type II (Baldridge et al. 2008; Morello et al. 2006). Recently, recessive mutations in *SERPINH1* (MIM# 600943) encoding a chaperone-like protein for collagens, heat shock protein 47 and in *SP7/Osterix* (MIM# 606633) encoding an osteoblast-specific transcription factor have been identified in patients with types III and IV, respectively (Christiansen et al. 2010; Lapunzina et al. 2010).

Two copies of the α1 chain and one copy of the α2 chain form a core triple helix comprising 338 uninterrupted Gly-X–Y triplet repeats, where X is often proline and Y is often hydroxyproline. Gly repeats at every third position are essential for the stability of collagen because larger amino acids cannot be accommodated in the tightly packed core without disruption of the triple helix (Bodian et al. 2008). The most common mutations (>80%) affect one of the repeated Gly residues in the triple helix. More than 800 mutations in *COL1A1* and *COL1A2* are currently deposited in the human type I collagen mutation database (http://www.le.ac.uk/genetics/collagen/) (Dalgleish 1997; Marini et al. 2007). Clinical phenotypes may be determined by the chain in which the Gly substitution occurs, the position of the mutation within the chain and/or the nature of the mutant amino acids (Bodian et al. 2008; Marini et al. 2007; Rauch and Glorieux 2004), but we still cannot predict a clinical phenotype of a given mutation. On the other hand, mutations that create a premature stop codon within *COL1A1* mostly exhibit a milder OI type I. This is because a truncation mutation is unlikely to have a dominant negative effect, but the abundance of type I collagen chain is half of the normal (Marini et al. 2007; Rauch and Glorieux 2004).

Pre-mRNA splicing is regulated by intronic and exonic splicing *cis*-elements. Both constitutively and alternatively spliced exons harbor exonic splicing enhancers (ESEs) and silencers (ESSs). Splicing *trans*-factors are expressed in a developmental stage-specific and tissue-specific manner, and their expressions tightly regulate alternative splicing of an exon carrying ESEs/ESSs. A mutation in the coding region is predicted to exert its pathogenicity by compromising a functional amino acid, but nonsense, missense and even silent mutations potentially disrupt an ESE/ESS, thereby resulting in aberrant splicing (Cartegni et al. 2002, 2003). Indeed, more than 16–20% of exonic mutations are predicted to disrupt an ESE (Gorlov et al. 2003).

Exome resequencing is a powerful and efficient method to identify a novel gene associated with a rare monogenic disorder, especially when the number of unrelated patients or the number of family members of a patient are too small to apply linkage studies. Filtering against existing SNP database and the exomes of unaffected individuals can remove common variants to identify a causal gene. Ng et al. (2009) sequenced exomes of 12 humans, including four unrelated individuals with autosomal dominant Freeman-Sheldon syndrome (MIM# 193700) and eight HapMap individuals. They successfully identified mutations in *MYH3* (MIM# 160720) in all the affected individuals. Ng et al. (2010b) also sequenced exomes of four patients in three families with autosomal recessive Miller syndrome (MIM# 263750) and de novo identified compound heterozygous mutations in *DHODH* (MIM# 126064). Ng et al. (2010a) additionally sequenced exomes of ten unrelated patients with autosomal dominant Kabuki syndrome (MIM# 147920) and de novo identified nonsense or frameshift mutations in *MLL2* (MIM# 602113). Similarly, Lalonde et al. (2010) sequenced two unrelated fetuses with autosomal recessive Fowler syndrome (MIM# 225790) and de novo identified compound heterozygous mutations in *FLVCR2* (MIM# 610865).

In a Japanese family with OI type I, hyperuricemia cosegregated with OI. To our knowledge, association of hyperuricemia with OI has been reported in two families, in which two of three OI patients had gouty arthritis and hyperuricemia at young ages (Allen et al. 1955). Underexcretion of urate is causally associated with mutations in *UMOD* (MIM# 191845) encoding uromodulin (Hart et al.

2002) as well as with SNPs in three genes: *SLC2A9* (MIM# 606142) encoding glucose transporter 9 (Doring et al. 2008; Vitart et al. 2008), *ABCG2* (MIM# 603756) encoding ATP-binding cassette subfamily G member 2, a urate transporter (Dehghan et al. 2008; Kolz et al. 2009; Stark et al. 2009; Woodward et al. 2009), and *SLC22A12* (MIM# 607096) encoding URAT1, a renal urate-anion exchanger (Graessler et al. 2006; Tabara et al. 2010). On the other hand, overproduction of urate is caused by mutations in *PRPS1* (MIM# 311850) encoding PRPP synthetase I (Roessler et al. 1993) and *HPRT1* (MIM# 308000) encoding hypoxanthine guanine phosphoribosyltransferase 1 (Gibbs and Caskey 1987).

We here identified a dominant missense mutation, c.3235G>A in *COL1A1* exon 45 predicting p.G1079S, in a Japanese family with OI type I and hyperuricemia, and analyzed the molecular bases of two clinical features. First, we tested if mild to lethal phenotypes of mutations in exon 45 of *COL1A1* were accounted for by preservation or disruption of an ESE/ESS element, and found that ESE/ESS elements were not involved in disease severities. Second, we traced a cause of the hyperuricemia by exome resequencing of two siblings and found that a missense mutation in *GPATCH8* encoding the G patch domain-containing protein 8 close to *COL1A1* cosegregated with hyperuricemia.

Patients and methods

Samples and ethical considerations

We obtained blood from each family member and isolated genomic DNA (gDNA) from 2 ml of peripheral blood using the QIAamp DNA Blood Midi Kit (Qiagen) according to the manufacturer's instructions. We also obtained skin biopsy of an affected individual (II-3) of a Japanese family (F1) and cultured non-transformed fibroblasts for splicing and sequencing analysis. Informed consent was obtained from all family members. The studies have been approved by the Institutional Review Boards of the Nagoya University, the University of Verona and the McGill University. Clinical features and mutational analyses have been previously reported in the Italian and Canadian families (Mottes et al. 1992; Roschger et al. 2008).

Microsatellite analysis of *COL1A1* and *COL1A2* to identify a mutation in the Japanese family

We genotyped all family members for three microsatellite markers flanking *COL1A1* (D17S1293, −16 Mbp; D17S1319, −14 kbp; and D17S788, 2 Mbp). As no annotated microsatellite markers were available close to *COL1A2*, we posted three new microsatellite markers to DDBJ (AB499843, −17 kbp; AB499844, 29 kbp; and AB499845, 123 kbp) and analyzed them in the family. We fluorescently labeled the 5′ end of each forward primer with 5FAM (Sigma-Aldrich), and amplified microsatellite markers with the HotStarTaq Plus Master Mix (Qiagen) using gDNA and primers indicated in Supplementary Table 1.

We mixed 1.5 μl of 20-times diluted PCR product with 0.5 μl of GeneScan-500 ROX Size Standard (Applied Biosystems) and 24.5 μl of formamide, and incubated the mixture at 95°C for 3 min. The mixture was run by capillary electrophoresis on an ABI PRISM 310 Genetic Analyzer and was analyzed with the GeneScan and GeneMapper software (Applied Biosystems).

Sequence analysis of *COL1A1*

After the microsatellite analysis suggested that *COL1A1* was more likely to be a causative gene, we amplified all exons and flanking intronic regions of ~40 bp, as well as 5′ and 3′ UTRs of *COL1A1* from gDNA of II-3 by PCR. We performed the dye terminator cycle sequencing reaction with the GenomeLab DTCS Quick Start Kit (Beckman Coulter) and ran on the CEQ 8000 Genetic Analysis System (Beckman Coulter) according to the manufacturer's instructions. We compared the chromatograms with the GenBank reference sequences of *COL1A1* gDNA using the Mutation Surveyor software version 2.61 (SoftGenetics). We numbered *COL1A1* mutations with the translation initiator methionine as amino acid +1, and the A of the ATG codon as nucleotide +1 according to the Human Genome Variation Society (http://www.hgvs.org/mutnomen/recs.html). We numbered exons according to the human type I collagen mutation database (http://www.le.ac.uk/genetics/collagen/), in which *COL1A1* exon 33 is named *COL1A1* exon 33–34 to match the exonic annotations of *COL1A2*.

Allele-specific primer (ASP)-PCR to trace the *COL1A1* mutation

We traced the mutation in family members using ASP-PCR. The wild-type ASP was 5′-TCCCGCCGGTCCT GTAGG-3′, and the mutant ASP was 5′-TCCCGCCGG TCCTGTAAG-3′, where the mutated nucleotide is underlined, and an artificially introduced mismatch is shown in bold. The reverse primer was 5′-GCCACGGTGAC CCTTTATGC-3′.

Prediction of effects of mutations on pre-mRNA splicing

Five missense mutations in exon 45 of *COL1A1* cause mild to lethal OI phenotypes (Fig. 2a) (Constantinou et al. 1989;

Hartikka et al. 2004; Lund et al. 1997; Marini et al. 2007; Mottes et al. 1992; Roschger et al. 2008). We predicted the effects on pre-mRNA splicing of 18 sequence variants with or without each mutation in the presence or absence of each of two SNPs (rs1800215 and rs1800217) in exon 45 of *COL1A1* (Fig. 2b) using five Web-based programs: ESEfinder 3.0 (http://rulai.cshl.edu/cgi-bin/tools/ESE3/esefinder.cgi?process=home) (Cartegni et al. 2003), ESR-search (http://ast.bioinfo.tau.ac.il/) (Goren et al. 2006), FAS-ESS (http://genes.mit.edu/fas-ess/) (Wang et al. 2004), PESXs (http://cubweb.biology.columbia.edu/pesx/) (Zhang and Chasin 2004; Zhang et al. 2005), and RESCUE-ESE (http://genes.mit.edu/burgelab/rescue-ese/) (Fairbrother et al. 2002). We also predicted the effects of the mutations on splice site strength of the 18 sequence variants using two Web-based programs: the NetGene2 Server (http://www.cbs.dtu.dk/services/NetGene2/) (Brunak et al. 1991; Hebsgaard et al. 1996) and the Splice Site Prediction by Neural Network (http://www.fruitfly.org/seq_tools/splice.html) (Reese et al. 1997).

Splicing analysis of fibroblasts of the OI patient (II-3)

We first examined splicing of *COL1A1* exon 45 in the patient's fibroblasts. We extracted total RNA from cultured fibroblasts of II-3 using Trizol reagent (Invitrogen) and synthesized cDNA using the oligo$(dT)_{12-18}$ primer (Invitrogen) and the ReverTra Ace reverse transcriptase (Toyobo). We examined skipping of *COL1A1* exon 45 using 5′-GGTTCCCCTGGACGAGAC-3′ on exon 43 and 5′-TCCAGAGGGACCTTGTTCAC-3′ on exon 47. We also sequenced RT-PCR products as described above to scrutinize splicing consequences. As skipping of exon 45 results in an in-frame deletion of 54 nucleotides, we did not downregulate the nonsense-mediated mRNA decay (NMD) before harvesting cells.

COL1A1 minigene constructs

We amplified exons 44–46 and the intervening introns of *COL1A1* (Fig. 2b) by PCR. The PCR primers introduced a *Hin*dIII site and the Kozak consensus sequence of 5′-CCACCATG-3′ to the 5′ end, as well as a TAA stop codon and a *Bam*HI site at the 3′ end of the PCR product, so that the minigene transcript is tolerant to NMD (Ohno et al. 2003). We inserted the PCR product into the pcDNA3.1(+) mammalian expression vector (Invitrogen) and confirmed the lack of PCR artifacts by sequencing the entire insert. We next constructed 17 variant minigenes using the QuikChange site-directed mutagenesis kit (Stratagene) (Fig. 2b). We again confirmed presence of the introduced mutations and absence of artifacts by sequencing the entire inserts.

Splicing assays of *COL1A1* exon 45

We transfected 500 ng of a minigene construct into 50% confluent HEK293 cells in a 12-well plate using the FuGENE 6 transfection reagent (Roche Applied Science) according to the manufacturer's instructions. After 48 h, we extracted total RNA from HEK293 cells and synthesized cDNA as described above. To prevent amplification of the endogenous *COL1A1*, we used generic primers of 5′-TTAATACGACTCACTATAGGGAGACC-3′ and 5′-TTAAGGAGGGCCAGGGGG-3′ located on pcDNA3.1. Untransfected cells were used as a negative control.

Founder analysis of three families with *COL1A1* c.3235G>A

To examine if the *COL1A1* c.3235G>A mutation arose from a common founder in the Japanese, Italian (Mottes et al. 1992) and Canadian (Roschger et al. 2008) families, we genotyped three microsatellite markers flanking *COL1A1* described above and sequenced an intragenic SNP (rs2075554) of *COL1A1* in the Italian and Canadian families (Fig. 1).

Sequence analysis of *PRPSAP1* and *PRPSAP2*

To seek for a responsible gene for hyperuricemia, we sequenced the entire coding regions of *PRPSAP1* and *PRPSAP2* on chr 17 using cDNA synthesized from cultured fibroblasts of II-3.

Resequencing of exome-enriched DNA

As we found no mutation in *PRPSAP1* and *PRPSAP2*, we enriched exonic regions of genomic DNA of II-2, II-3 and VIII-2 using the SureSelect human all exon kit v1 (Agilent Technologies) that covers 1.22% (34 Mbp) of the human genome. We sequenced 50 base pairs of each tag in a single direction using a quarter of a cell of the SOLiD 3 Plus system (Life Technologies) for each sample.

For II-2, II-3 and VIII-2, we obtained 79.1, 68.6 and 109.9 $\times$ 10^6 tags of 50-bp SOLiD reads and mapped 2.18 (69.6%), 1.87 (68.5%) and 3.37 (76.5%) Gbp to the human genome hg19/GRCh37, which yielded a mean coverage of 64.1, 55.1 and 99.0, respectively. Among the mapped tags, 70.1, 72.0 and 73.1% were located on the SureSelect exome probes. Among the 34-Mbp regions where the exome probes were designed, 3.4, 3.6 and 3.5% of nucleotides

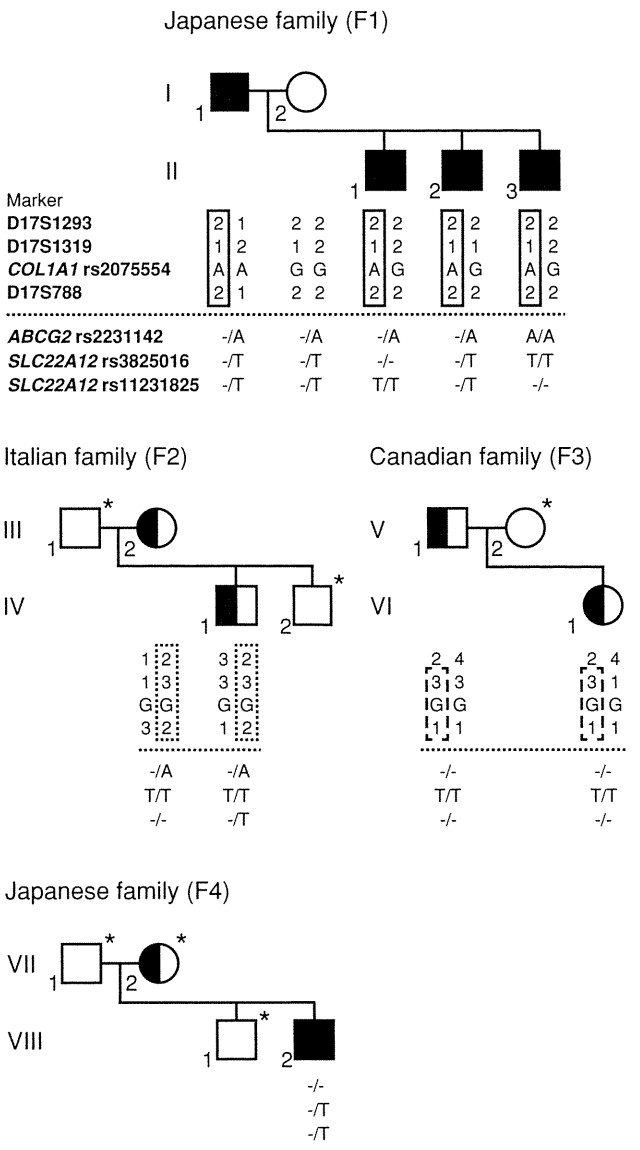

Fig. 1 Pedigrees, haplotypes and genotypes of the Japanese (F1 and F4), Italian (F2) and Canadian (F3) families. Patients in F1, F2 and F3 have c.3235G>A predicting p.G1079S in *COL1A1*. A patient in F4 has c.577G>T predicting p.G193C in *COL1A2*. *Closed symbols* indicate patients with OI and with hyperuricemia. *Half-shaded symbols* represent OI without hyperuricemia. *Asterisks* indicate that DNA sample is not available for our studies. Clinical subtypes are all type I except for the Canadian father (V-1), who exhibits type IV. In F1, hyperuricemia cosegregates with OI. Genotypes of three microsatellite markers (D17S1293, −16 Mbp; D17S1319, −14 kbp; and D17S788, 2 Mbp) flanking *COL1A1* and an SNP (rs2075554) in intron 11 of *COL1A1* are indicated for all the available members in F1, F2, and F3. F1, F2 and F3 carry their unique haplotypes (shown by *solid*, *dotted* and *broken boxes*, respectively). The D17S1293 genotype in F3 is not informative and is not boxed. Genotypes of hyperuricemia-associated SNPs (rs2231142, rs3825016 and rs11231825) are indicated at the bottom of each pedigree tree

were not sequenced at all. Search for single nucleotide variants (SNVs) and indels with Bioscope 1.2.1 (Life Technologies) detected 52,436, 56,941 and 60,303 SNVs/indels. SNVs and indels were compared to dbSNP Build 132.

Analysis of variants in *KRBA2, ZPBP2* and *GPATCH8*

To trace if variants in *KRBA2*, *ZPBP2* and *GPATCH8* co-segregated with hyperuricemia, we analyzed all family members in the Japanese family (F1) by capillary sequencing.

We traced two variants, *ZPBP2* c.206C>T and *GPATCH8* c.2935G>C, in the Italian and Canadian families and 100 normal human genomes using ASP-PCR. The forward primers of *ZPBP2* and *GPATCH8* were 5′-CGT GTCTTCAGCACAAAATGG-3′ and 5′-AGAAGCCGTA GCACCACT**C**C-3′, respectively. The reverse primers were 5′-GGCCCAATCCATAAGTA**C**AT-3′ and 5′-CCCA TGATCTCTTCCTGGAG-3′, respectively. The mutated nucleotide is underlined, and an artificially introduced mismatch is shown in bold.

To search for the identified variants in *ZPBP2* and *GPATCH8* in normal controls, we mapped 50 Tibetan exome reads (SRA accession number SRP002446) (Yi et al. 2010) to a 200-bp region spanning c.206C>T in exon 3 of *ZPBP2* and a 200-bp region spanning c.2935G>C in exon 8 of *GPATCH8* with the bowtie alignment tool version 0.12.7 (Langmead et al. 2009) using default parameters.

We analyzed amino acid conservations of *ZPBP2* and *GPATCH8* using the evolutionary annotation database, Evola, at the H-Inv DB (http://www.h-invitational.jp/evola/). We also predicted functional effects of amino acid substitutions using two Web-based programs: PolyPhen-2 (http://genetics.bwh.harvard.edu/pph2/) (Adzhubei et al. 2010) and SIFT (http://sift.jcvi.org/) (Kumar et al. 2009).

Results

Hyperuricemia cosegregated with OI type I in the Japanese family (F1)

In a Japanese family (F1), a father (age 56 years) and his three sons (ages 29, 26 and 23 years) had OI type I with blue sclera, dentinogenesis imperfecta and joint laxity (Fig. 1). Two sons (II-1 and II-3) had histories of more than ten fractures before age 13 years, but the father (I-1) and another son (II-2) experienced no bone fracture. One son (II-1) had hearing loss from age 10 years likely due to fractures or deformities of small bones in the middle ear and had hip joint deformities due to repeated femoral fractures. Interestingly, all the affected members had hyperuricemia of ~8 mg/dl that was diagnosed at ages 15–30 years. One son (II-3) had a gout attack, and the other two (I-1 and II-1) had urinary stones. Hyperuricemia is currently well controlled by medication in all the members.

Heteroallelic c.3235G>A mutation in *COL1A1* in the Japanese family (F1)

Genotypes of three microsatellite markers flanking *COL1A1* cosegregated with the OI phenotype in F1 (Fig. 1), whereas genotypes of three markers flanking *COL1A2* did not (data not shown). We thus sequenced the entire exons and the flanking noncoding regions and identified a heteroallelic c.3235G>A mutation in exon 45 and a heteroallelic G/A SNP (rs2075554) in intron 11 of *COL1A1*. The c.3235G>A mutation predicts p.G1079S. We genotyped c.3235G>A in family members by ASP-PCR, and found that all affected members were heterozygous for c.3235G>A (Fig. 1).

Phenotypic variability of osteogenesis imperfecta is not accounted for by disruption of splicing *cis*-elements

In addition to c.3235G>A, four more mutations and two SNPs have been reported in *COL1A1* exon 45 with variable phenotypes ranging from mild type I to perinatal lethal type II (Fig. 2a) (Constantinou et al. 1989; Hartikka et al. 2004; Lund et al. 1997; Marini et al. 2007; Mottes et al. 1992; Roschger et al. 2008). We thus hypothesized that disruption or de novo generation of a splicing *cis*-element determines the clinical phenotype. The five mutations and two SNPs in *COL1A1* exon 45 were predicted to affect 16 putative splicing *cis*-elements by ESEfinder, ESRsearch and PESXs (Table 1). FAS-ESS and RESCUE-ESE predicted no splicing *cis*-elements. All the five mutations with or without two SNPs in *COL1A1* exon 45 variably but slightly weaken acceptor and/or donor splice site strengths according to the NetGene2 (Table 2). The splice site prediction by neural network also predicted that c.3235G>A generates a weak cryptic splice acceptor site in *COL1A1* exon 45 (Table 2). We first examined cultured fibroblasts of II-3 by RT-PCR and found that the *COL1A1* c.3235G>A mutation did not induce aberrant splicing of *COL1A1* (data not shown). NMD was unlikely to have masked aberrant splicing, because we observed heterozygous peaks at c.3235G>A in sequencing the RT-PCR product. We next constructed 18 *COL1A1* minigenes with or without each of the five mutations in the presence or absence of each of the two SNPs (Fig. 2b). RT-PCR analysis of transfected HEK293 cells showed that all minigene constructs gave rise to a single fragment of 336 bp, indicating that splicing was not affected in any mutations or SNPs (Fig. 2c).

Japanese (F1), Italian (F2) and Canadian (F3) families with *COL1A1* c.3235G>A share no founder haplotype

We previously reported *COL1A1* c.3235G>A in the Italian and Canadian families (Marini et al. 2007; Roschger et al. 2008). Although we have not measured serum urate concentrations in these families, gout or urinary stone has not been documented in either family, which suggests that hyperuricemia is not simply due to c.3235G>A.

To pursue if a gene responsible for hyperuricemia is on the same chr as *COL1A1*, we looked for a founder haplotype for c.3235G>A in three families by genotyping three microsatellite markers flanking *COL1A1* (D17S1293, −16 Mbp; D17S1319, −14 kbp; and D17S788, 2 Mbp) and an SNP (rs2075554) in intron 11 of *COL1A1*. The analysis revealed that each family carried a unique haplotype and shared no founder haplotype (Fig. 1). Thus, the mutation is likely to have occurred independently in three ethnic groups. Alternatively, c.3235G>A is an ancient founder mutation, and subsequent multiple recombinations and divergence of microsatellite repeats have obscured a founder effect. In either case, lack of a found haplotype supports the notion that a gene responsible for hyperuricemia is potentially but not necessarily linked to *COL1A1*.

Hyperuricemia is not caused by mutations in *PRPSAP1* or *PRPSAP2*

We thus first looked into candidate genes for hyperuricemia on chr 17 where *COL1A1* (17q21.31–q22) is located. Two candidate genes for hyperuricemia are on chr 17: *PRPSAP1* (MIM# 601249) at 17q24–q25 encoding PAP39 (Ishizuka et al. 1996) and *PRPSAP2* (MIM# 603762) at 17p12-p11.2 encoding PAP41 (Katashima et al. 1998). PAP39 and PAP41 are subunits of phosphoribosylpyrophosphate (PRPP) synthetase that leads to urate production. No mutation has been reported in either gene in any diseases. We sequenced cDNAs of *PRPSAP1* and *PRPSAP2* in II-3, but found no mutation in either gene. As we detected no heterozygous SNPs in *PRPSAP1* and *PRPSAP2*, a mutant allele carrying a premature stop codon might have been missed due to mRNA degradation by NMD.

Resequencing of exomes reveals hyperuricemia-associated SNPs

We next traced a causative gene for hyperuricemia in two siblings (II-2 and II-3) by exome resequencing with the SureSelect human all exon kit v1 (Agilent) and with the SOLiD 3 Plus sequencer (Life Technologies).

We similarly analyzed an unrelated Japanese male (22-year-old) with OI type I and hyperuricemia (VIII-2 in F4 in Fig. 1). His hyperuricemia was by chance detected at age 14 years when he had fractures. His hyperuricemia has been well controlled by medication since then. Exome resequencing of VIII-2 disclosed a novel heteroallelic c.577G>T mutation in *COL1A2* exon 12 predicting

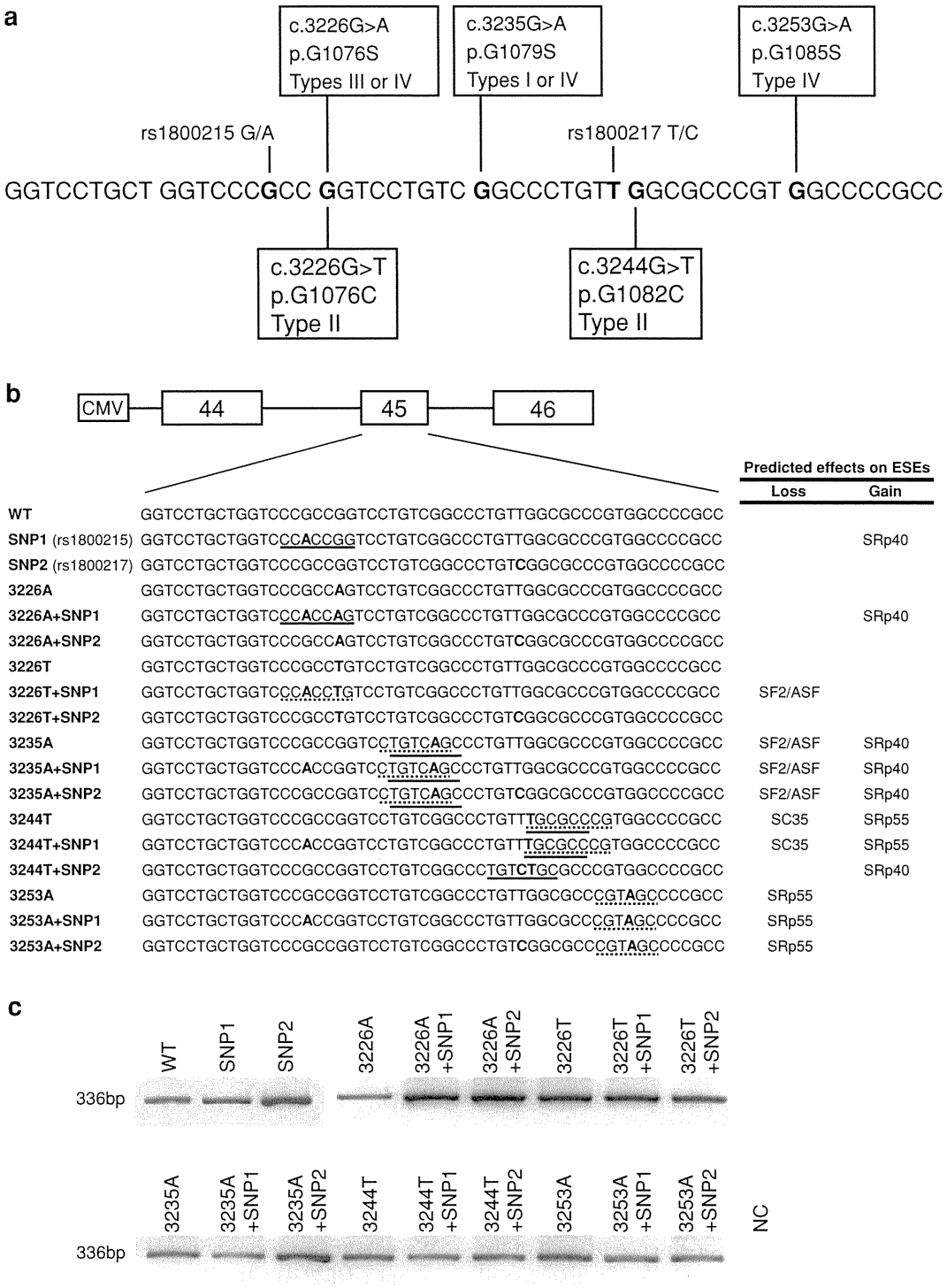

Fig. 2 Splicing assays of *COL1A1* minigenes in HEK293 cells. **a** Positions and phenotypes of OI mutations in *COL1A1* exon 45. Mutations above the wild-type sequence exhibit non-lethal phenotypes, whereas those below the sequence cause a lethal phenotype. **b** Schematic representation of *COL1A1* minigenes. Sequences of mutant minigenes are indicated *below*. Substituted nucleotides are shown in *bold*. Predicted gain and loss of splicing *cis*-elements by ESEfinder (Cartegni et al. 2003) are indicated by *solid* and *dotted underlines*, respectively. **c** RT-PCR of minigenes introduced into HEK293 cells. All constructs show a single fragment of 336 bp, indicating that *COL1A1* exon 45 is not skipped in any constructs. Untransfected cells are used as a negative control (*NC*)

p.G193C. We confirmed the mutation by capillary sequencing. Family samples were not available for our analysis.

In F1, a probability that three siblings inherited an identical allele from the father is $(1/2)^3 = 12.5\%$, which indicates that the causative gene is anywhere in the